JOURNAL OF MATERIALS SCIENCE 16 (1981) 2883–2889

Long-term ageing characteristics of some commercial nickel–chromium–molybdenum alloys

H. M. TAWANCY
High Technology Materials Division, Cabot Corporation, Kokomo, Indiana 46901, USA

The long-term ageing characteristics of some commercial Ni–Mo–Cr alloys (the high-temperature HASTELLOY* alloy S and the corrosion resistant HASTELLOY alloys C-4 and C-276) at 810 K were investigated. It was found that the three alloys undergo the following long-range ordering reaction: disordered f c c lattice → ordered orthorhombic, Pt_2Mo-type superlattice. Ordering was found to cause considerable strengthening without severe loss of tensile elongation. Deformation in the ordered state occurred predominantly by twinning. The corrosion rates of alloys C-4 and C-276 in boiling sulphuric–ferric sulphate solution did not seem to be greatly affected by the long-range ordering reaction. In addition to ordering, the three alloys were also found to undergo grain boundary reactions. The resulting phase in alloys S and C-4 assumed a dispersed morphology and was identified as carbide, probably of the Type $M_{12}C$. In alloy C-276, however, which contains higher amounts of iron and tungsten, the boundary precipitate was in the form of a continuous layer consisting of $M_{12}C$ and Mu-phase. This could account for the reduced tensile elongation of alloy C-276 relative to alloys S and C-4 and also to its high corrosion rate.

1. Introduction

The Ni–Mo–Cr system forms the basis for a number of commercial alloys among which are the high temperature HASTELLOY* alloy S and the corrosion resistant HASTELLOY alloys C-4 and C-276. Alloy C-276 contains higher amounts of iron and tungsten than alloy C-4 (see Table I). It is important for a number of applications to determine the long-term ageing response of these alloys at various temperatures. Recently, the source of strengthening in alloy S upon long-term ageing at 810 K was found to be a long-range ordering reaction whereby the disordered fcc lattice transforms into an ordered orthorhombic Pt_2Mo-type superlattice [1, 2]. In view of the similarity in chemical compositions among these alloys, the same source of strengthening might also be expected in alloys C-4 and C-276. The objective of this investigation was to compare the response of these alloys to identical ageing conditions. Emphasis was placed on the ordering reaction, grain boundary precipitation and the corresponding effects on tensile properties, corrosion rates and fracture characteristics.

2. Experimental procedure

The alloys investigated were of commercial grade and their chemical compositions are given in Table I.

The final heat treatment of alloys S and C-4 consisted of annealing at 1340 K (1950° F) followed by air cooling and water quenching respectively. The treatment of alloy C-276 consisted of annealing at 1395 K (2050° F) followed by water quenching. All heat treatments were carried out in a continuous bright anneal furnace. In each case, the resulting microstructure consisted of an essentially single phase. Metallographic and stan-

*HASTELLOY is a registered trademark of Cabot Corporation.

0022–2461/81/102883–07$02.70/0 © *1981 Chapman and Hall Ltd.*

TABLE I Chemical compositions (wt%)

Alloy	Element												
	Ni	Cr	Mo	Fe	W	Co	Mn	Si	Al	La	Ti	S	C
S	Bal.	15.14	14.23	1.00	0.25	0.23	0.55	0.32	0.17	0.022	0.01	0.005	0.007
C-4	Bal.	15.68	15.43	1.65	0.23	0.81	0.14	0.04	0.28	–	0.23	0.007	0.006
C-276	Bal.	15.73	15.77	5.58	3.30	1.85	0.49	0.04	0.26	–	0.01	0.006	0.006

TABLE II Room-temperature tensile properties

Alloy	Condition	0.2% yield strength, MPa	(ksi)	Ultimate tensile strength, MPa	(ksi)	Tensile elongation (%) (50.8 mm gauge length)
S	Annealed	436	(63)	892	(129)	58
	Annealed + aged 8000 h at 810 K	823	(119)	1286	(186)	42
C-4	Annealed	380	(55)	851	(123)	55
	Annealed + aged 8000 h at 810 K	802	(116)	1363	(197)	35
C-276	Annealed	360	(52)	802	(116)	62
	Annealed + aged 8000 h at 810 K	775	(112)	1245	(180)	28

dard tensile specimens were aged for 8000 h at 810 K. All tensile tests were performed at room temperature. Thin foils for transmission electron microscopy and diffraction work were prepared by jet polishing in a solution of 33% nitric acid in methanol at about 243 K. All the foils were examined at an accelerating voltage of 100 kV.

3. Experimental results and discussion

3.1. Tensile properties and corrosion rates

Table II shows typical room-temperature tensile properties in the annealed and aged conditions. It can be seen that 0.2% yield strength of each alloy had nearly doubled relative to the annealed condition. Although alloys S and C-4 retained about 70% of their tensile elongation, alloy C-276 retained only 45%.

Typical corrosion rates of alloys C-4 and C-276 in boiling sulphuric–ferric sulphate solutions are given in Table III. The test solution used is known

TABLE III Corrosion rates of alloys C-4 and C-276

Alloy	Condition	Corrosion rate ($mm\ y^{-1}$)
C-4	Annealed	3.3
	Annealed + aged 8000 h at 810 K	5.4
C-276	Annealed	5.7
	Annealed + aged 8000 h at 810 K	67.5

to dissolve molybdenum-rich phases such as carbides and Mu-phase [3]. It will be shown later that the high corrosion rate of alloy C-276 and its reduced tensile elongation relative to alloys S and C-4 could be due to precipitation of a continuous grain boundary layer consisting of a carbide and Mu-phase.

3.2. Long-range ordering

Electron diffraction patterns derived from matrixes of the three alloys in the aged condition were identical in that they contained extra weaker reflections at every 1/3 ⟨220⟩ and 1/3 ⟨420⟩ face centred cubic reflection as shown in Fig. 1. This characterizes an orthorhombic Pt_2Mo-type superlattice where six crystallographically equivalent variants can be directly derived from the fcc lattice by stacking of atomic layers on either {420} or {220} planes [4]. Bright-field images derived from regions corresponding to the patterns of Fig. 1 showed a fine-scale "mosaic" assembly as exemplified by Fig. 2. The size of the ordered domains as revealed by dark-field imaging using superlattice reflections was found to be of the order of 10 nm as shown in Fig. 3. X-ray microanalysis using scanning transmission electron microscopy showed no significant difference between bulk chemical composition and that of the ordered domains which indicated a generalized ordering reaction. This is in agreement with a similar study conducted on HASTELLOY alloy C-276

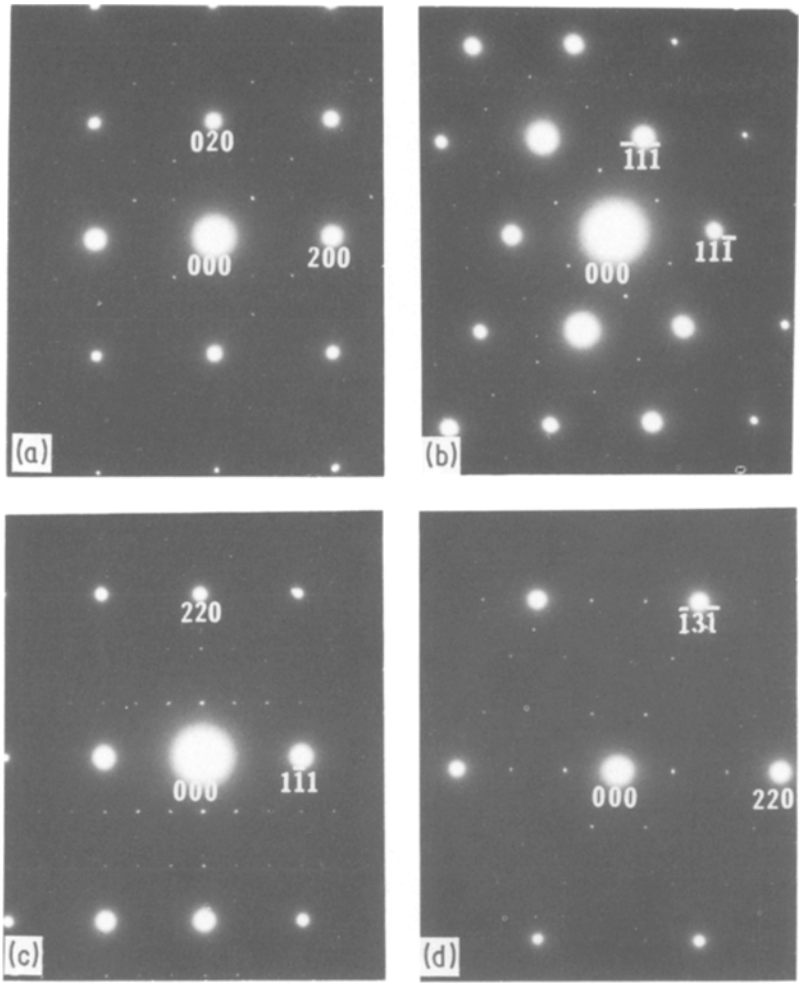

Figure 1 Selected-area electron diffraction patterns representative of HASTELLOY alloys S, C-4 and C-276 (aged 8000 h at 810 K), orthorhombic Pt_2Mo-type superlattice. The patterns are indexed in terms of f c c notations. (a) 0 0 1, (b) 0 1 1, (c) $\bar{1}$ 1 2 and (d) $\bar{1}$ 1 4.

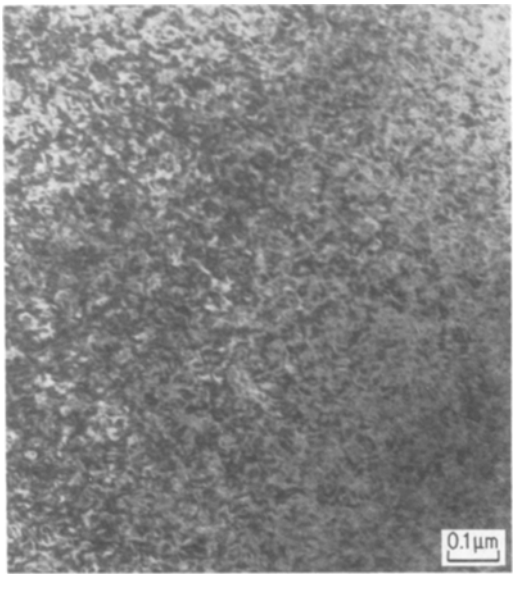

Figure 2 Bright-field TEM micrograph showing a fine scale "mosaic" assembly in the ordered state.

[5]. Due to the small domain size and the large volume fraction, it was not possible to determine whether the structure was effectively single-phase or two-phase. The above observations demonstrated the close similarity among the alloys investigated in that they all undergo a long-range ordering reaction whereby:

disordered f c c lattice → ordered orthorhombic Pt_2Mo-type superlattice.

Also, ordering did not seem to affect the corrosion rates of alloys C-4 and C-276 as they appeared to be in the same state of ordering, yet their corrosion rates varied widely (Table III).

3.3. Deformation substructure in the ordered state

Examination of the substructure of tensile-tested specimens in the ordered state showed extensive $\{1\,1\,1\}_{fcc}$ deformation twins, as shown in Fig. 4.

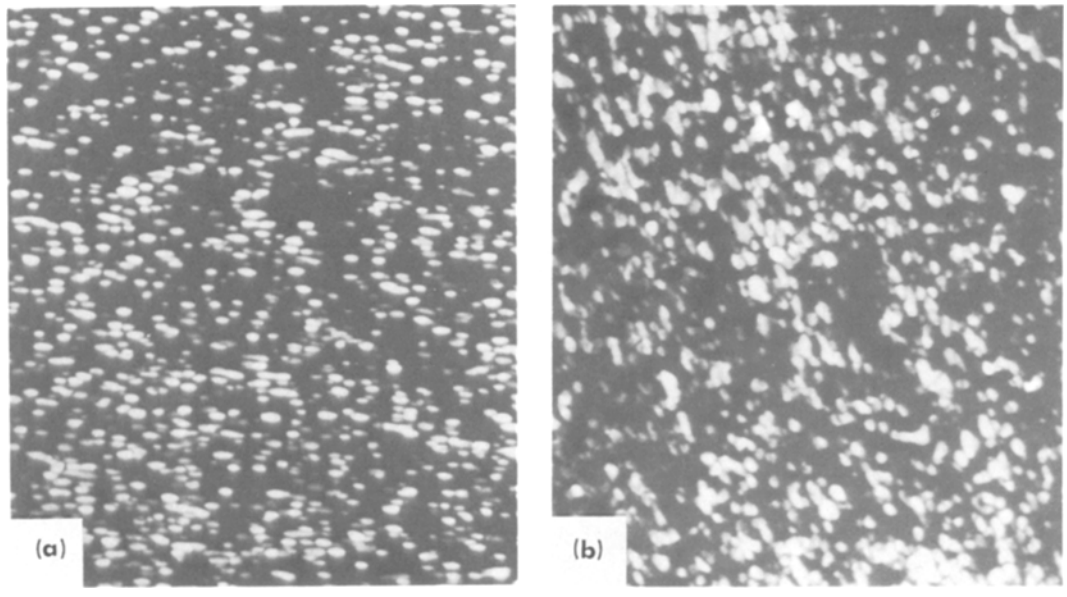

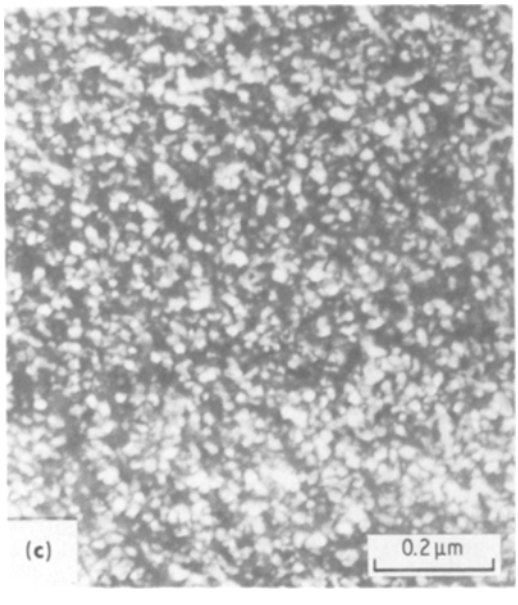

Figure 3 Dark-field images formed with 1/3 ⟨2 2 0⟩ reflections to reveal the ordered domains. (a) HASTELLOY alloy S, (b) HASTELLOY alloy C-4 and (c) HASTELLOY alloy C-276.

Fig. 5 shows the typical appearance of the ordered domains within the twins. This observation demonstrated that deformation by twinning was energetically more favourable than that by motion of slip dislocations. Such behaviour could be interpreted in terms of the effect of the structural change (f c c → orthorhombic) associated with ordering on both slip and twinning systems. It was shown that while such a change makes ten of the twelve f c c slip systems energetically unfavourable, it makes only two of the twelve twinning systems unfavourable [5]. The observed strengthening upon ordering could then be due to a change in deformation mode from slip to twinning which usually requires greater stress.

3.4. Grain boundary precipitation

Fine grain boundary precipitates were observed in aged samples of the three alloys investigated. Alloys S and C-4 were similar in that the grain boundary precipitate assumed a dispersed morphology and had an f c c structure with a lattice constant of about 1.086 nm as determined by electron diffraction (Fig. 6). This data and the rela-

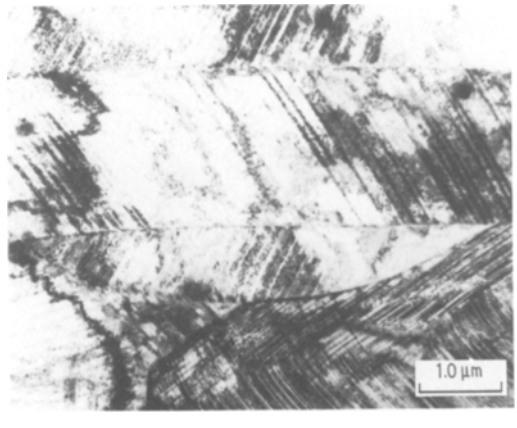

Figure 4 Bright-field TEM micrograph showing extensive deformation twins characteristic of tensile-tested specimens in the ordered state.

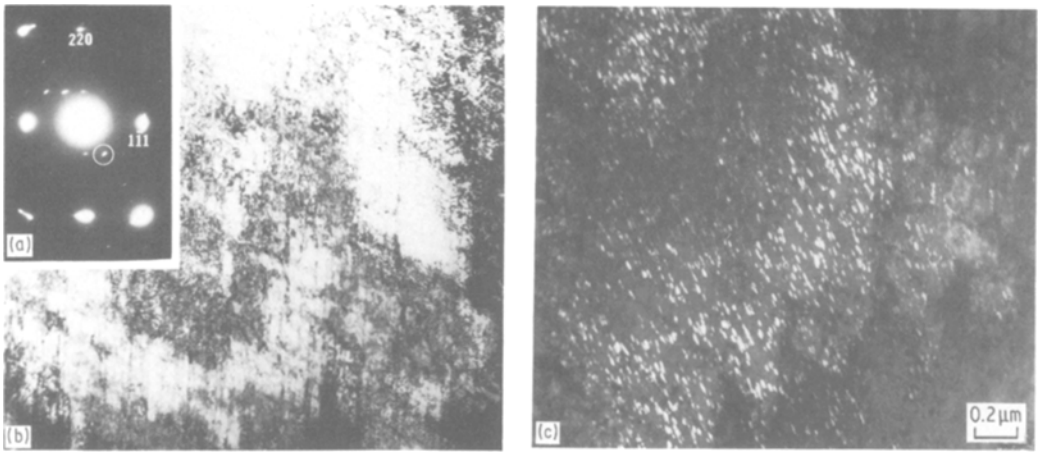

Figure 5 Appearance of ordered domains in tensile-tested specimens. (a) Selected area electron diffraction pattern near [0 1 1], (b) bright-field image and (c) dark-field image formed with the encircled superlattice reflection in (a).

tively low carbon contents of these alloys (Table I) suggested that the boundary phase is a carbide of the Type $M_{12}C$ as were found in the Ni–Mo–C system [6] and HASTELLOY alloys N [7] and B-2 [8]. In alloy C-276, however, the boundary precipitate assumed a continuous layer consisting of two phases (Fig. 7). One phase was found to be the same as that in alloys S and C-4, i.e. $M_{12}C$, and the other was a Mu-phase (isomorphous with Fe_7Mo_6). It is known that Mu-phase can nucleate in carbides rich in Mu-forming elements, e.g. M_6C and $M_{12}C$ which are both molybdenum-rich, provided that other Mu-forming elements such as iron and tungsten are present in sufficient quantities. These conditions seemed to have been satisfied in alloy C-276. Accordingly, the reduced tensile elongation and high corrosion rate of alloy C-276 in the aged condition could be due to the presence of that continuous grain boundary layer.

3.5. Tensile fracture characteristics

Examination of the tensile fracture surfaces of the three alloys in the aged condition revealed a mixture of intergranular and transgranular fracture modes as shown in Fig. 8. Voids could have been

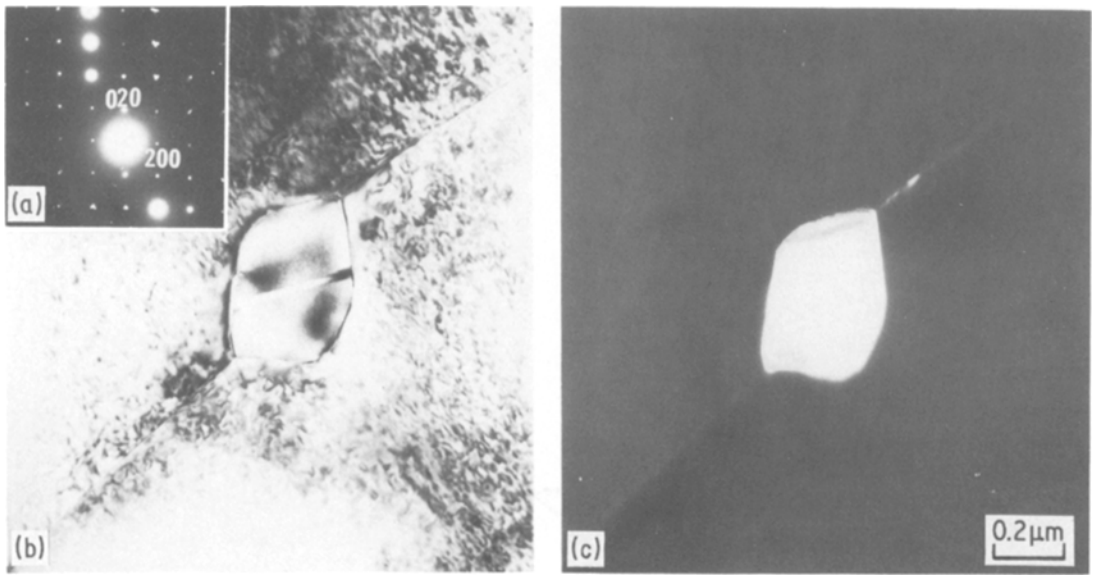

Figure 6 Grain boundary carbide particle characteristic of HASTELLOY alloys S and C-4. (a) [0 0 1] selected area diffraction pattern, (b) bright-field image and (c) dark-field image formed with (0 2 0) reflection.

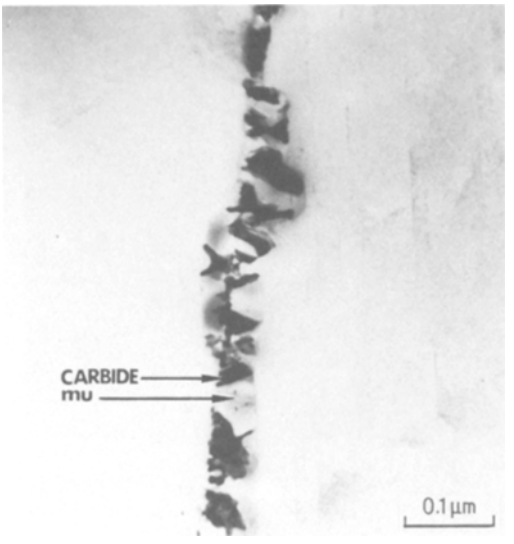

Figure 7 Bright-field TEM micrograph showing characteristic continuous grain boundary precipitate in HASTELLOY alloy C-276.

nucleated at twin–twin intersections as well as twin–grain boundary intersections. It was noted, however, that intergranular fracture was more pronounced in alloy C-276. This could be due to the observed continuous grain boundary precipitate.

4. Conclusions

The long-term ageing characteristics of some Ni–C–Mo alloys at 810 K were investigated, and it could be concluded that:

(1) They undergo a long-range ordering reaction whereby the disordered f c c lattice is transformed into an ordered orthorhombic Pt_2Mo-type superlattice.

(2) Ordering causes considerable strengthening without severe loss in tensile elongation.

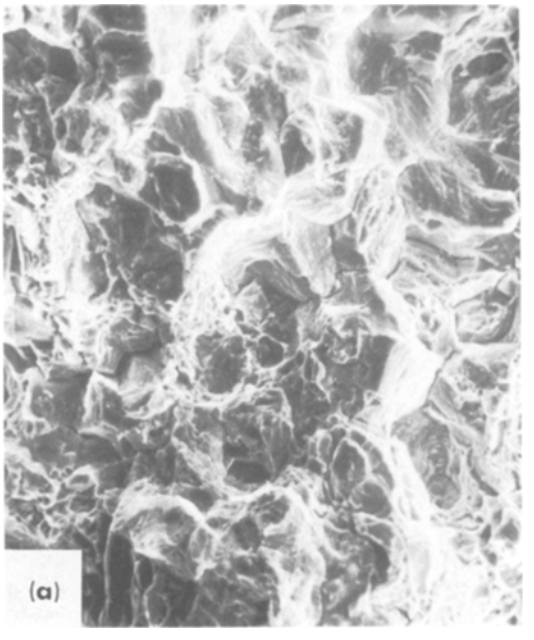

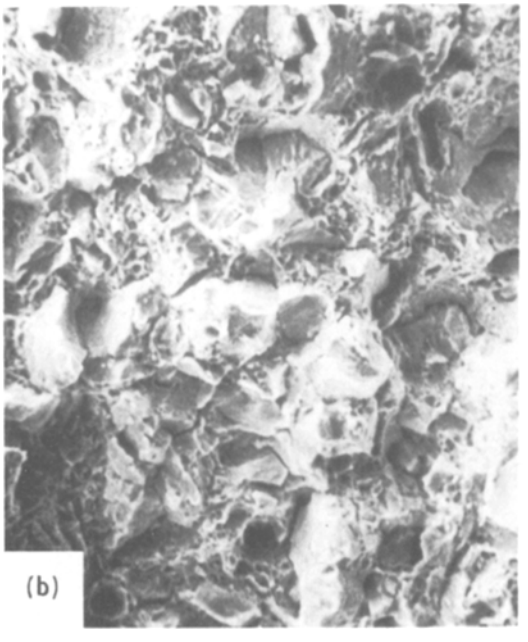

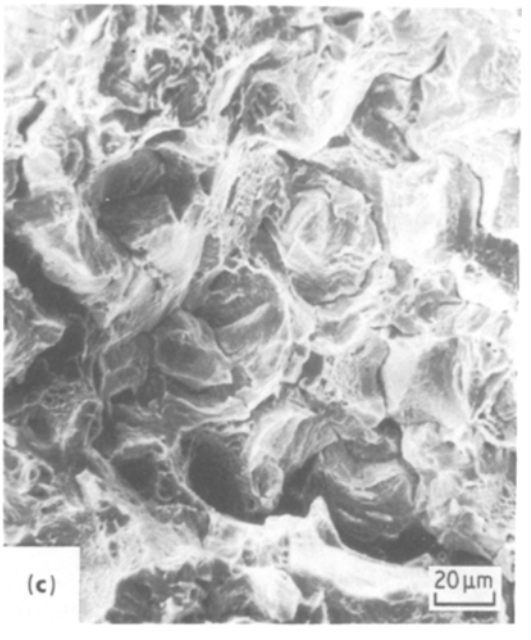

Figure 8 Scanning electron micrographs showing characteristic tensile fracture surfaces of ordered specimens. (a) HASTELLOY alloy S, (b) HASTELLOY alloy C-4 and (c) HASTELLOY alloy C-276.

(3) Deformation in the ordered state occurs predominantly by twinning rather than by slip.

(4) The alloys investigated also undergo grain boundary reactions that result in dispersed carbide phase probably of the Type $M_{12}C$ in alloys S and C-4 and a continuous layer consisting of $M_{12}C$ and Mu-phase in alloy C-276. The latter could lead to the observed reduced tensile elongation and high corrosion rate of alloy C-276.

References

1. H. M. TAWANCY, *Met. Trans.* **11A** (1980) 1764.
2. S. J. MATTHEWS, Proceedings of the 3rd International Conference on Superalloys, Seven Springs, 1976 (Claitor's Publishing Division, Baton Rouge, 1976) p. 215.
3. M. A. STREICHER, *Corrosion* **32** (1976) 79.
4. S. K. DAS and G. THOMAS, *Phys. Stat. Sol. (a)* **21** (1974) 177.
5. P. D. JOHNSON, PhD thesis, University of Notre Dame, Indiana, 1980.
6. A. C. FRAKER and H. H. STADELMAIR, *Trans. AIME* **245** (1969) 847.
7. J. M. LEITNAKER, G. A. POTTER, D. J. BRADLEY, J. C. FRANKLIN, and W. R. LAING, *Met. Trans.* **9A** (1978) 397.
8. H. M. TAWANCY, *J. Mater. Sci.* **16** (1981) 1117.

Received 22 January and accepted 6 April 1981.